https://doi.org/10.48048/tis.2023.6670

Synthesis and Characterization of TiO_2-Chitosan Beads and Its Application as A Degradation Agent of Methylene Blue

Eka Apriliani Rosdiana, Nor Basid Adiwibawa Prasetya* and Gunawan Gunawan

Department of Chemistry, Faculty of Sciences and Mathematics, Diponegoro University, Semarang, Indonesia

(*Corresponding author's e-mail: nor.basid.prasetya@live.undip.ac.id)

Received: 26 January 2023, Revised: 11 March 2023, Accepted: 27 March 2023, Published: 27 April 2023

Abstract

Dye waste is an environmental problem that has a negative impact on the ecosystem. One way to overcome this is by chemically degrading dyes using photocatalyst materials. TiO_2 is one of the photocatalysts that can be synthesized by utilizing microwave radiation which is transferred directly to the material. This method takes a short amount of time so it can be completed in a very short time. TiO_2 powder has the disadvantage that it is difficult to separate from the waste solution. TiO_2 can be modified into beads by utilizing chitosan to produce TiO_2-chitosan beads (TCB). In this research, the synthesis of TiO_2 was carried out using microwave, followed by modification with chitosan to produce TCB and then its application in the degradation of methylene blue dye waste at various pH, concentration and contact time variations. Material characterization was carried out by determining the surface area of the material using Brunauer-Emmet-Teller (BET), band gap energy with UV-Vis Diffuse Reflectance Spectrocopy (UV-Vis DRS), crystal phase with X-Ray Diffraction (XRD), and surface morphology with Scanning Electron Microscope (SEM). The results showed that the synthesized TiO_2 has anatase crystalline phase with an average crystal size of 18.85 nm and a bandgap energy of 3.16 eV. The TCB surface morphology indicated the successful impregnation of TiO_2 on the chitosan. This study showed that the optimum performance of TCB was at pH 11 within 5 min and kinetic analysis results follows 2nd order.

Keywords: Photocatalyst, Microwave, TiO_2, Chitosan, Beads, Methylene blue

Introduction

A number of wastes industries such as plastics, textiles, cosmetics, food, and others contain high concentrations of dyes. The textile industry is known as the most intensive chemical industry in the world using dyes. The textile industry is responsible for an extensive list of environmental impacts [1]. The textile dyes, along with a large number of industrial pollutants, are highly toxic and potentially carcinogenic [2]. The removal of dyes from wastewater is therefore a serious ecological problem worldwide.

One of the industrial dyes is methylene blue (MB) which is an important basic dye in the dyeing process in the textile industry. MB is also used in various applications such as chemical, biological, medical science and textile industries [3]. The textile industry usually releases large amounts of MB dyes in natural water sources, which pose a health threat to humans and microbes [4]. MB has toxic, carcinogenic, and non-biodegradable properties and can cause serious threats to human health and be destructive to the environment [5]. The Center for Drug Evaluation and Research [6] proved that MB has carcinogenic properties. In addition, MB causes several risks to human health such as respiratory problems, stomach disorders, blindness, and digestive and mental disorders [7]. MB also causes nausea, diarrhea, vomiting, cyanosis, shock, gastritis, jaundice, methemoglobinemia, tissue necrosis, increased heart rate, causes premature cell death in tissues and skin/eye irritation [8]. MB also reduces light penetration and is a toxic supply to the food chain for organisms [9]. Cationic dyes such as methylene blue are more toxic than anionic dyes.

Chemical treatment of industrial dye waste can be carried out through degradation using photocatalyst materials, such as $BiVO_4$, ZnO, TiO_2 and others. Pure $BiVO_4$ has low photocatalytic activity which is caused by poor adsorption performance and difficulties in migration and separation of electron-hole pairs [10]. ZnO showed rather poor photocatalytic activities due to their limited photo response ranges under visible light [11]. One of the other photocatalyst materials, titanium dioxide (TiO_2), has gained great attention as a promising photocatalyst due to its beneficial properties among the other photocatalysts, such as excellent optical and electronic properties, high chemical stability, low cost, non-toxicity, and eco-

friendliness [12]. In contrast, titanium dioxide is very responsive to UV light, electron and hole pairs are generated by UV radiation and encourage chemical reactions on the surface of the material [13]. However, the use of TiO_2 photocatalysts as powder still has drawbacks, especially after photocatalyst process is completed where TiO_2 is difficult to separate in liquid media [14]. The weakness of using TiO_2 in powder form is the formation of agglomeration which affects the performance of the photocatalyst [15]. In the treatment of textile dye waste, TiO_2 powder is easily coagulated in solution so that the solution becomes cloudy and absorption of light in the degradation process will be less effective [16].

The important role of TiO_2 in waste treatment makes research regarding the synthesis of TiO_2 important. TiO_2 can be synthesized into nanomaterials which have attractive properties and can be widely applied. Various methods have been used to synthesize TiO_2 nanoparticles including direct precipitation [17], sol gel [18], sonochemical method [19], milling and coprecipitation [20], hydrolysis method [21], solvothermal [22], and microwave [23]. Microwaves method utilizes microwave radiation which is transferred directly to the material. This method provides uniform energy distribution within the sample, better reproducibility and excellent control over experimental parameters. Compared to other methods, microwaves method offers relatively short time so it can be completed in a few minutes.

The separation, recovery, and re-use of TiO_2 nanoparticles is also a major constraint to its industrial applications [24]. Therefore, synthesizing TiO_2 in the form of beads offers an ease of re-collection and reuse. Various materials have been used for the manufacture of TiO_2 beads, including alginate [25], hexadecylamide [26], and phosphopeptides [27]. In this study, chitosan-modified TiO_2 or also called TCB (TiO_2-chitosan beads) was used. Chitosan was chosen because of its abundance, biocompatible and biodegradable [28]. Chitosan is a derivative compound resulting from the deacetylation process of chitin which is contained in many marine animals such as shrimp and crabs [29]. Chitosan is a cationic biopolymer containing 2 free and active functional groups, namely hydroxyl and amine groups. These 2 functional groups are also available for cross-linking [30]. Therefore, it is necessary to conduct research to examine the performance of TCB.

In this study, the researchers synthesized TiO_2 using microwave, synthesized modified TiO_2 in the form of beads with the addition of chitosan as a support because of the convenience for re-collection and reuse. In the application of TCB photocatalyst, the optimum conditions were sought to degrade methylene blue with variations in pH, time and concentration.

Materials and methods

Materials and apparatus

Titanium isopropoxide (TTIP) (p.a., Sigmaaldrich), isopropyl alcohol (IPA) (p.a., merck), distilled water, chitosan, acetic acid p.a., glutaraldehyde (p.a., Nitra Kimia), sodium hydroxide (NaOH), methylene blue (MB), hydrochloric acid (HCl) (p.a., merck), microwave 700 W, UV lamp (T5UVC, 8 watt, 253.7 nm), oven, furnace, UV reactor, magnetic stirrer, centrifugal, ultrasonic, UV-Vis spectrophotometer.

Preparation of TiO_2

Titanium isopropoxide (TTIP, 0.5 M) in isopropyl alcohol (IPA, 100 mL) was stirred with a magnetic stirrer for 15 min, then distilled water (30 mL) was added dropwise and the mixture was continously stirred for 30 min. The mixture was exposed to microwave irradiation in 700 W for 5 min. Next, the mixture was left at room temperature for 24 h, then centrifuged. The mixture was dried in an oven at 80 °C for 12 h, then calcined at 500 °C for 2 h.

Preparation of TCB

The synthesis of TiO_2-chitosan beads material (TCB) was carried out by mixing chitosan (0.5 g) with 10 % acetic acid (10 mL), then TiO_2 (0.2 g) was added and the mixture was ultrasonicated for 15 min. Glutaraldehyde (1.6 mL) was then added and the mixture was left for 4 h at room temperature. Next, the mixture was dripped into 100 mL of NaOH with a concentration of 0.25 mol/L. TCB obtained was then washed with distilled water and dried in an oven at 60 °C.

Characterization

Determination of the surface area of the material was carried out with Brunauer-Emmet-Teller (BET), measurement of band gap energy with UV-Vis Diffuse Reflectance Spectrocopy (UV-Vis DRS), and Scanning electron microscopy with energy dispersive X-ray spectroscopy (SEM-EDX) for morphological structure identification, and X-Ray Diffraction (XRD), for phase identification of crystalline materials. Based on the XRD characterization data, crystal size can be estimated using the Scherrer formula.

$$D = \frac{K\alpha}{\beta\cos\theta}$$

D = crystal size (nm)
K = constant (0.94)
λ = wavelength of X-ray used (nm)
β = Full Width of Half Maximum (FWHM)/Integral Breadth of the peak
θ = diffraction angle

while the data obtained from UV-Vis DRS is used to calculate the band gap energy with the Kubelka-Munk equation:

$$F(R) = \frac{K}{S} = \frac{(1-R)^2}{2R}$$

F(R) = kubelka-munk factor
K = absorption coefficient
S = scattering coefficient
R = measured reflectance value

$$F(R)^2 = \frac{A^2}{S^2}(hv - E_g)$$

A = proportional constant
E_g = band gap energy

Effect of pH on photodegradation

Testing for TCB in degradation of methylene blue solution was carried out with several pH variations, which were pH 2, 4, 11, and 13. A total of 25 ml of methylene blue solution was added with 0.01 g TCB then put into a UV photoreactor (**Figure 1**) for 3 min and measured its absorbance.

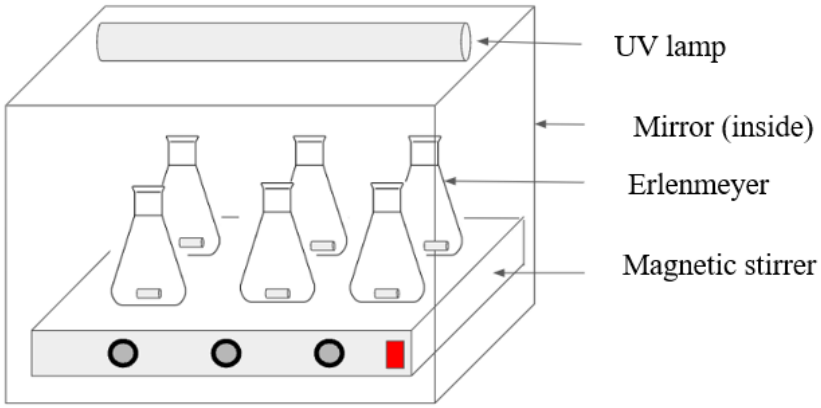

Figure 1 UV photoreactor design.

Effect of concentration on photodegradation

Testing for TCB in degradation methylene blue solution was carried out by adding 25 mL of methylene blue solution with various concentrations of 2, 4, 6, 8, and 10 ppm with 0.01 g TCB then put into the UV reactor and measured the absorbance.

Effect of contact time on photodegradation

TCB testing on degradation of methylene blue solution was carried out with several contact times at 4 different pH conditions, which were pH 2, 4, 11, and 13, with variations in contact time of 1, 3, 5, 10, and 15 min. A total of 25 mL of methylene blue solution was added with 0.01 g of TCB and then put into the UV reactor and the absorbance was measured.

Results and discussion

Characterization of TiO_2 and TCB

Crystal analysis using XRD (X-ray Diffraction) aims to determine the crystal structure of the synthesized TiO_2 and TCB. Based on the analysis and diffractogram in **Figure 2**, the TiO_2 d-spacing values are obtained which can be used to determine the shape of TiO_2 crystals by comparing the d-spacing values of the analysis results with standard TiO_2 crystal data interpretation cards. The comparison is shown in **Table 1**. Based on the comparison in **Table 1**, it can be concluded that the synthesized TiO_2 has anatase crystalline phase.

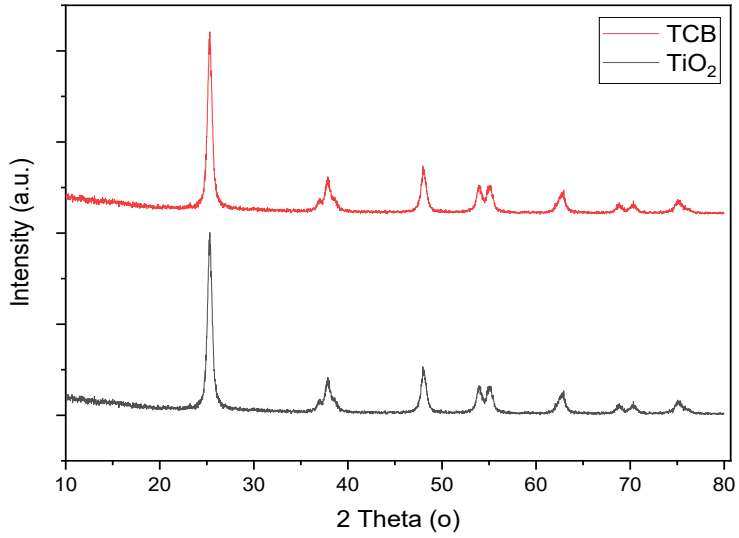

Figure 2 Diffractogram of TiO_2 and TCB catalyst analysis results using XRD.

Table 1 The d-spacing value of the analysis results and interpretation card of TiO_2 crystal data.

TiO_2 d-spacing data interpretation card		d-spacing TiO_2 synthesis	Result
Anatase	Rutile		
3.52	3.247	3.5151526	Anatase
2.378	2.487	2.370740819	Anatase
1.892	2.188	1.889226878	Anatase
1.699	2.054	1.698334452	Anatase
1.666	1.687	1.665390703	Anatase
1.481	1.623	1.477788969	Anatase
1.364	1.479	1.364104919	Anatase
1.338	1.359	1.338717544	Anatase
1.265	1.346	1.263741286	Anatase

From the calculation results, the crystal size and the average crystal size are 18.85 nm. This crystal size indicates that the synthesized TiO_2 is of nanoparticle size because based on the literature the size of nanoparticles is between 1 - 100 nm [31]. With this nanoparticle size, TiO_2 photocatalyst performance is more optimum because the surface area that interacts is larger.

Table 2 TiO_2 crystal size based on the Scherrer formula.

2θ	FWHM Left [°2Th.]	Crystal size (nm)
25.3167	0.4723	17.23945021
37.0482	0.3542	23.65435223
37.9214	0.4330	19.39968225
48.1250	0.3149	27.62889051
53.9449	0.3542	25.16629342
55.1015	0.7085	12.64697687
62.8325	0.6298	14.78080937
68.7619	0.5510	17.46991973
70.2555	0.7872	12.33914511
75.1124	0.5510	18.18712227

Crystal analysis using XRD was also performed for the synthesized TCB. In the analysis of the 2θ value and the TCB diffractogram, **Figure 2**, there was no clear change in the diffraction pattern when compared with pure TiO_2 raw material. This shows that the processing method of TiO_2 chitosan beads has no effect on the crystal phase of TiO_2 nanoparticles.

The characterization test using UV-DRS aims to determine the bandgap energy of TiO_2 and TCB. The band gap energy greatly affects the performance of TiO_2, which is a semiconductor. By plotting F(R) against hv and extrapolating the linear region, it is possible to determine the value of hv at F(R) = 0, which is the bandgap energy (Eg) of the absorbing species. Based on the extrapolation results as shown in **Figure 3** through the kubelka Munk equation approach, the gap energies of TiO_2 and TCB are 3.21 and 3.16 eV.

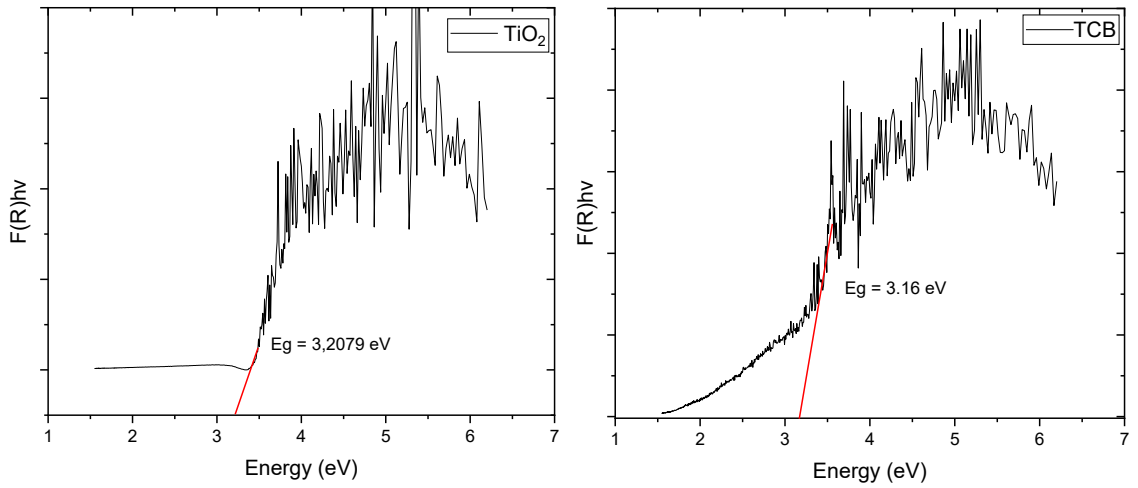

Figure 3 Graph F(R) to energy (a) TiO_2, and (b)TCB.

BET Adsorption-desorption with nitrogen at a temperature of 77.3 K was carried out to determine the interaction between the adsorbent and the adsorbate. The curve in **Figure 4** further illustrates the BET equation where there is completion of the first layer adsorption before adsorption of the second and subsequent layers begins. Adsorption does not lead to saturation in this curve. This type is the multilayer adsorption isotherm model, type II. This type is the normal form of isotherms on non-porous (non-porous) adsorbents or large porous solids (macropores) with sizes larger than 50 nm which exhibit monolayer - multilayer adsorption [32].

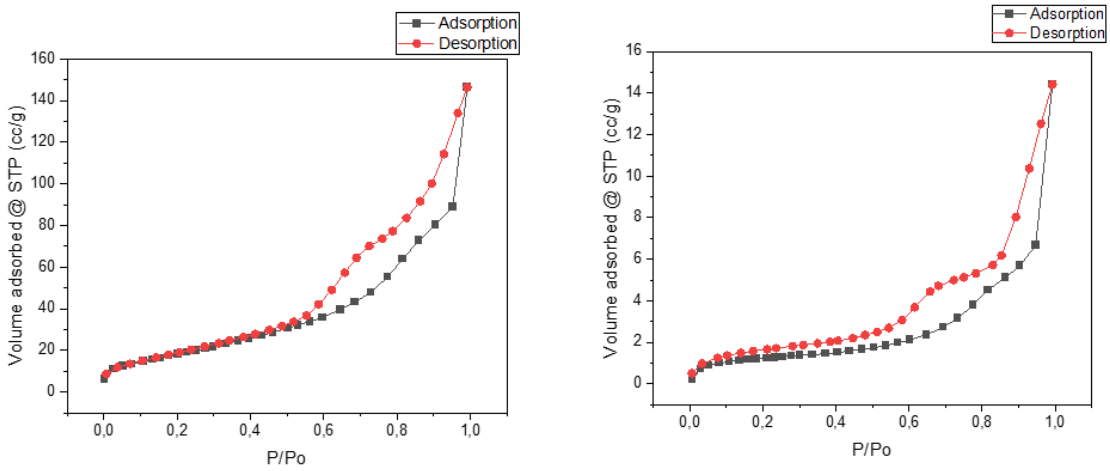

Figure 4 Adsorption-desorption curve (a) TiO_2, and (b) TCB.

Based on the analysis of the TiO_2 and TCB micropores, the porosity data for the 2 samples were obtained as shown in **Table 3**. The data shows that TCB has lower surface area and pore radius but still keep similar pore volume than those of TiO_2.

Table 3 Porosity data of TiO_2 and TCB from adsorption isotherm at 77.3 K.

Sample	Surface area of micropore (S_{D-R}) (m^2/g)	Pore volume (V_{D-R}) (cc/g)	Pore radius (D_{D-R}) (Å)	Adsorption energy (kJ/mol)
TiO_2	71.918 m^2/g	2.264×10^{-1}	62.9489	2.652
TCB	4.273 m^2/g	2.230×10^{-1}	10.4360	2.587

Characterization with SEM-EDX aims to observe the morphology and total composition of synthesized TiO_2 and TCB. SEM analysis was carried out at 1000× magnification as shown in **Figure 5**. It clearly shows the morphological changes of TiO_2 and TCB. TiO_2 looks very smooth, while TCB looks aggregated and coated with small particles around it. The surface morphology of TCB shows TiO_2 impregnation on the chitosan surface.

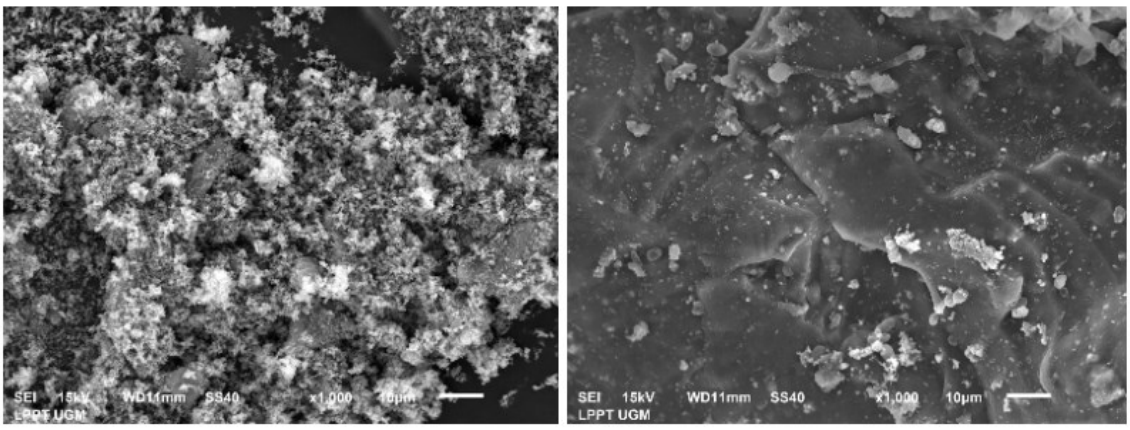

Figure 5 SEM-EDX (a) TiO_2, and (b)TCB.

TiO_2 and TCB materials were analysed using Attenuated Total Reflectance-Fourlier Transform Infrared (ATR-FTIR) to determine the presence of certain functional groups present in the synthesized material. The results of functional group analysis on TiO_2 and TCB materials are shown in **Figure 6**.

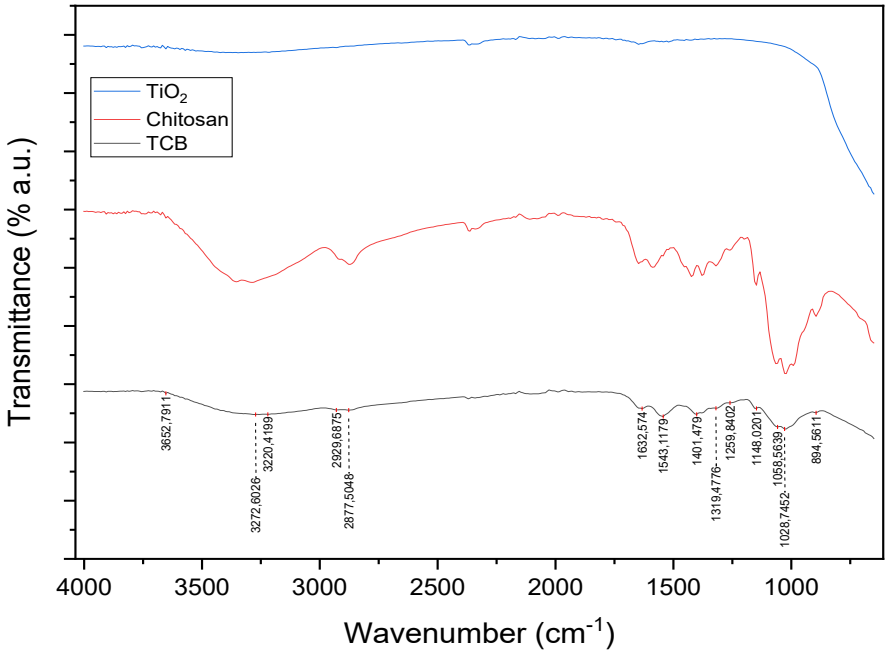

Figure 6 ATR-FTIR Spectra of TiO_2, Chitosan, and TCB.

Table 4 Functional group analysis on TiO_2, chitosan, and TCB.

Wave number	Functional group
3272	Interaction between NH_2 and OH with TiO_2
2923-2872	C–H (symmetrical and asymmetrical vibration), TiO_2-OH
1735-1730	O–C–NH_2
1632	N–H (primary amine), interaction Ti^{4+} with –NH_2, C=N
1370-1420	C–O–C (stretching), N=O (vibration), –NH (deformation), CH_3
1330-1420	O–H (bending)
1259	Bond Ti–OH and Ti–O
1029-1152	C–N (bending vibration), C–O–C (asymmetrical strain vibration of the glycosidic bond, Ti–O–C (bending), Bond Ti–OHz

The incorporation of TiO_2 into the chitosan matrix mainly occurs in the amorphous region of chitosan, strengthening the hydrogen bonds at wave number 3272 cm^{-1}, in the CS–TiO_2 complex, as shown in **Table 4**. The stretching of the C–O, amino, and hydroxyl groups is strongly bound to the TiO_2 nanoparticles which drives the formation of the CS–TiO_2 composite through the electrostatic interaction of the N–H–O–Ti bonds. In addition, a peak also appears at 1058 cm^{-1} which corresponds to the Ti–O–C bond, indicating that CS and TiO_2 have been chemically bound and not simply adsorbed into the CS matrix as a result of the cross-linking process and the complex composite structure. However, during CS–TiO_2 preparation, the tendency of TiO_2 to agglomerate was prevented because chitosan masked the Van der Waals effect on TiO_2

nanoparticles, due to the immobilization of nano-TiO_2 in the chitosan matrix. The band at 1637 - 1715 cm^{-1} corresponds to the C=N bond which is the result of chitosan cross-linking with the addition of glutaraldehyde.

Photocatalytic activity test

The maximum wavelength is determined to know the point of the maximum absorption area of the standard solution concentration. This measurement is carried out at the maximum wavelength so that the change in sample adsorption per unit concentration is the largest so that the sensitivity of the analysis becomes better and rearranging the wavelength will result in a small analysis error.

Determination of the maximum wavelength was measured using methylene blue solution with a concentration of 10 ppm at a wavelength of 200 - 800 nm by measuring absorbance scanning data using a UV-Vis spectrophotometer. According to the results of the scanning data, the maximum wavelength for methylene blue at pH conditions 2, 4, 6, 8, 10, 11, 12, and 13 is 664 nm, as shown in **Figure 7**.

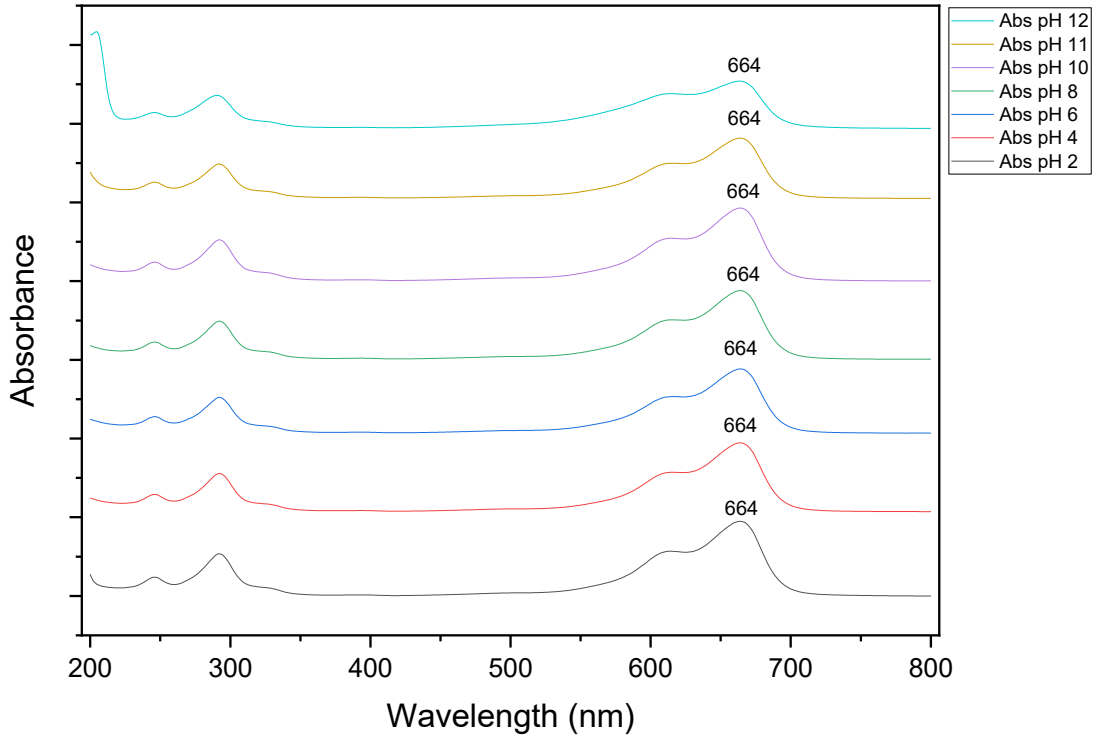

Figure 7 Graph of methylene blue scanning data at various pH variations at 200 - 800 nm.

Tests with variations in pH and time were carried out to determine the best pH and time conditions where TCB worked optimally as a methylene blue photocatalyst. Determination of the optimum pH condition is based on the smallest absorbance value measured using a UV-Vis spectrophotometer.

Based on the 4 pH variations that have been tested, for methylene blue only and methylene blue exposed to UV light as shown in **Figure 8**, the absorbance value is constant while the optimum absorbance is obtained at pH 11 for methylene blue substance with the addition of TCB accompanied by exposure to UV light and in the dark reaction. The final concentration of methylene blue and the percentage of degradation are shown in the graph of the relationship between the variation of pH and the percentage of degradation. As can be seen in the graph, the highest degradation percentage for methylene blue with the addition of TCB accompanied by exposure to UV light or in the dark reaction was at pH 11 for 5 min. The cationic nature of the MB dye is favored by the negatively charged TiO_2 surface due to the fact that the electrostatic interaction between TiO^- and MB^+ predominates [33]. Therefore, the best performance was observed at pH 11.

The optimum time conditions were obtained in the 5th min with percent degradation of 71.30 %. The addition of TCB accompanied by exposure to UV light in the 15th min showed a degradation percentage of 75.64 %.

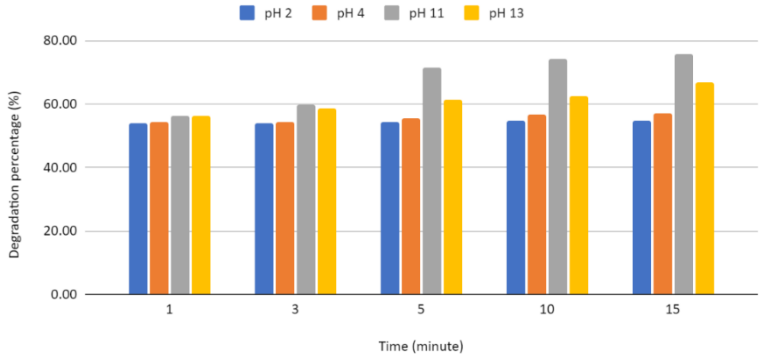

Figure 8 The effect of pH and time on the photodegradation performance of TCB by exposure to UV light.

In the test with varying concentrations of methylene blue, the optimum degradation percentage was obtained at a concentration of 2 ppm, with the addition of TCB and exposure to UV light, 92.74 % as shown in **Figure 9**.

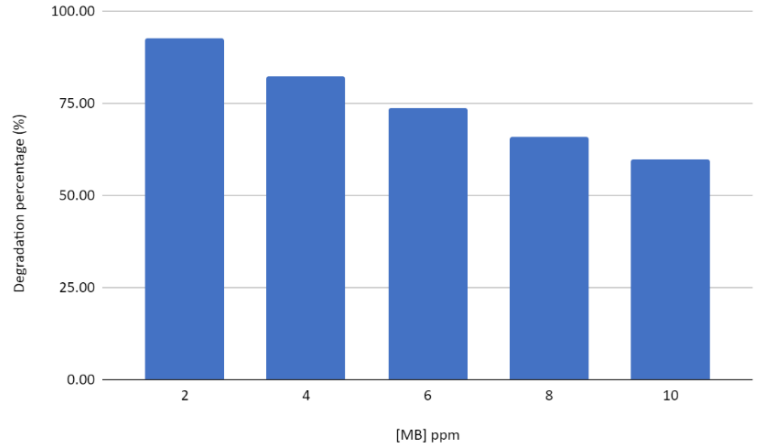

Figure 9 Graph of the effect of MB concentration on TCB photodegradation by exposure to UV light.

The results of variations in pH, time, and concentration of MB were used to determine the kinetics of the photocatalytic reaction between TCB accompanied by exposure to UV light to MB. Determination of the kinetics of this reaction can be carried out by several methods, such as the reaction mechanism method, the half-life method and the differential linear regression method [34]. In this study, the differential linear regression method was used for equations of order 0, order 1, and order 2.

The notation k can represent the photocatalytic rate constant, A_0 represents the initial concentration of the solution to be adsorbed and A_t represents the concentration of the solution to be adsorbed at time t. Determination of adsorption kinetics is carried out by stretching C_e (A_t), ln C_e $(ln$ $A_t)$, $1/C_e$ $(1/A_t)$ and $1/C_e^2$ $(1/A_t^2)$ data against t which will form a linear graph with a correlation value (R^2) certain.

Order 0 on the variation of pH and time

Determination of the order of variations in pH and contact time was carried out by linear regression using a zero-order equation in **Figure 10**, namely:

$A_t = A_0 - kt$

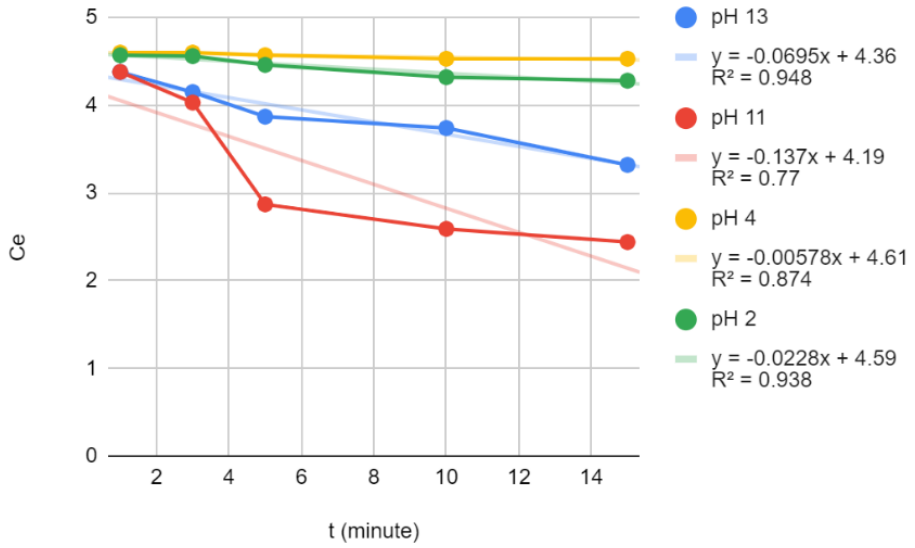

Figure 10 0 order linear graph of TCB photocatalysis against MB.

Order 1 on the variation of pH and time

Determination of the order of variations in pH and contact time was carried out by linear regression using a first order equation in **Figure 11**, namely:

A_0-ln A_t = kt

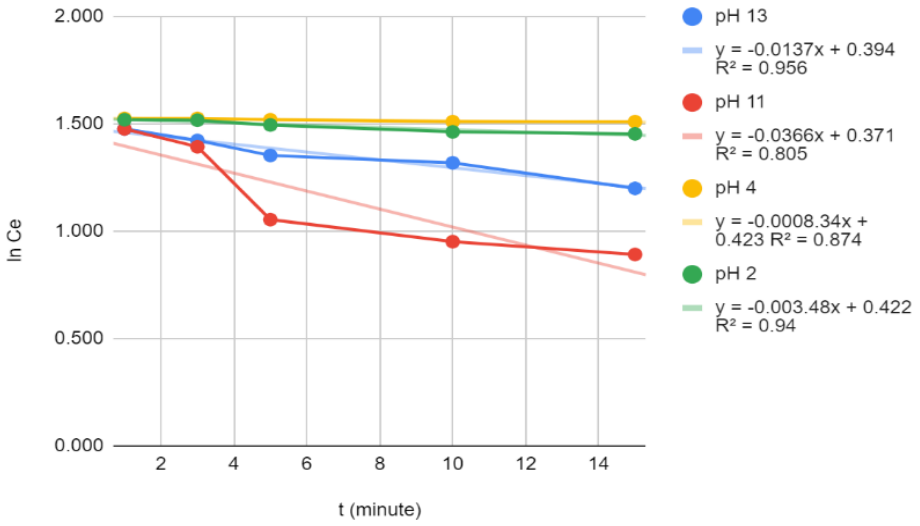

Figure 11 1st order linear graph of TCB photocatalysis against MB.

Order 2 on the variation of pH and time

Determination of the order of variations in pH and contact time was carried out by linear regression using a second order equation in **Figure 12**, namely:

A_t- A_0 = kt

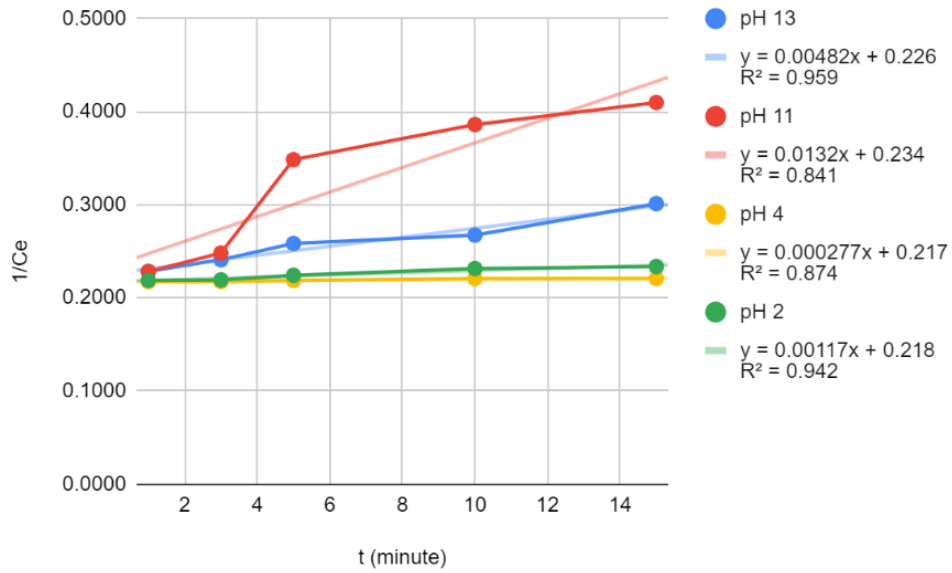

Figure 12 2nd order linear graph of TCB photocatalysis against MB.

Table 5 Kinetics of TCB photocatalyst with UV exposure to MB.

pH	Order	Linear equation	Kinetic parameters
13	0	y = –0.0695x + 4.36	R^2 =0.948 k = –0.0695
	1	y = –0.0137x + 0.394	R^2 = 0.956 k = –0.0137
	2	y = 0.00482x + 0.226	R^2 = 0.959 k = 0.00482
11	0	y = –0.137x + 4.19	R^2 = 0.77 k = –0.137
	1	y = –0.0366x + 0.371	R^2 = 0.805 k = –0.0366
	2	y = 0.0132x + 0.2342	R^2 = 0.841 k = 0.0132
4	0	y = –0.00578x + 4.61	R^2 = 0.874 k = –0.00578
	1	y = –0.000834x + 0.423	R^2 = 0.874 k = –0.000834
	2	y = 0.000277x + 0.217	R^2 = 0.874 k = 0.000277
2	0	y = –0.0228x + 4.59	R^2 = 0.938 k = –0.0228
	1	y = –0.00348x + 0.422	R^2 = 0.942 k = –0.00348
	2	y = 0.00117x + 0.218	R^2 = 0.942 k = –0.00117

Based on the results of the kinetic analysis in **Table 5**, the value of order 2 is obtained. This result is viewed from the correlation value of each order calculation where the R^2 value is the largest and close to 1st in the 2nd order calculation. This kinetic determination can also explain that the largest k value indicates the largest photolytic rate is in pH 11 condition.

Conclusions

TiO_2 photocatalyst material can be synthesized using the microwave method to produce nano-sized materials and can be modified using chitosan to produce TCB which is more easily separated from liquid than TiO_2. TCB composite material acts as an adsorbent as well as a photocatalyst for methylene blue. Chitosan is an excellent adsorbent and TiO_2 is a photocatalyst that can degrade methylene blue. TCB as a modified material is able to degrade methylene blue dye waste in the presence of UV light exposure optimally at pH 11 and 5 min with the kinetic analysis result follows 2nd order.

References

[1] SS Muthu. (2017). *Introduction*. *In*: SS Muthu (Ed.). Sustainability in the textile industry. Springer, Singapore, 2017.

[2] P Sharma, N Capalash and V Gupta. *Laccases and their role in bioremediation of industrial effluents*. *In*: R Chandra (Ed.). Advances in biodegradation and bioremediation of industrial waste. CRC Press, Boca Raton, 2015.

[3] D Pathania, S Sharma and P Singh. Removal of methylene blue by adsorption onto activated carbon developed from Ficus carica bast. *Arabian J. Chem.* 2017; **10**, S1445-S1451.

[4] Y Pang, ZH Tong, L Tang, YN Liu and K Luo. Effect of humic acid on the degradation of methylene blue by peroxymonosulfate. *Open Chem.* 2018; **16**, 401-6.

[5] L Sun, D Hu, Z Zhang and X Deng. Oxidative degradation of methylene blue via PDS-based advanced oxidation process using natural pyrite. *Int. J. Environ. Res. Publ. Health* 2019; **16**, 4773.

[6] AT Farrel. *Treatment of adults and children with acquired methemoglobinemia*. Center for Drug Evaluation and Research Application, Maryland, 2015.

[7] EA Abdelrahman, RM Hegazey and RE El-Azabawy. Efficient removal of methylene blue dye from aqueous media using Fe/Si, Cr/Si, Ni/Si, and Zn/Si amorphous novel adsorbents. *J. Mater. Res. Tech.* 2019; **8**, 5301-13.

[8] AH Jawad, AS Abdulhameed and MS Mastuli. Acid-factionalized biomass material for methylene blue dye removal: A comprehensive adsorption and mechanism study. *J. Taibah Univ. Sci.* 2020; **14**, 305-13.

[9] OE Ebi, AF Taiwo and AT Folorunsho. Kinetic modelling of the biosorption of methylene blue onto wild melon (*Lagenariasphaerica*). *Am. J. Chem. Eng.* 2018; **6**, 126-34.

[10] S Phanichphant, A Nakaruk, K Chansaenpak and D Chennai. Evaluating the photocatalytic efficiency of the $BiVO_4$/rGO photocatalyst. *Nat. Sci. Rep.* 2019; **9**, 16091.

[11] G Sodeifian and R Behnood, R. Hydrothermal Synthesis of N-Doped GQD/CuO and N-Doped GQD/ZnO Nanophotocatalysts for MB dye removal under visible light irradiation: Evaluation of a new procedure to produce N-Doped GQD/ZnO. *J. Inorg. Organomet. Polym. Mater.* 2020; **30**, 1266-80.

[12] HNC Dharma, J Jaafar, N Widiastuti, H Matsuyama, S Rajabsadeh, MHD Othman, MA Rahmad, NNM Jafri, NS Suhaimin, AM Nasir and NH Alias. A review of titanium dioxide (TiO_2-based photocatalyst for oilfield-produced water treatment. *Membranes* 2022; **12**, 345.

[13] CB Anucha, I Altin, E Bacaksiz and Stathopoulos. Titanium dioxide (TiO_2)-based photocatalyst materials activity enhancement for contaminants of emerging concern (CECs) degradation: In the light of modification strategies. *Chem. Eng. J. Adv.* 2022; **10**, 100262.

[14] R Li, T Li and Q Zhou. Impact of titanium dioxide (TiO_2) modification on its application to pollution treatment - a review. *Catalysts* 2020; **10**, 804.

[15] G Li, L Lv, H Fan, J Ma, Y Li, Y Wan and XS Zhao. Effect of the agglomeration of TiO_2 nanoparticles on their photocatalytic performance in the aqueous phase. *J. Colloid Interface Sci.* 2010; **348**, 342-7.

[16] H Dong, G Zeng, L Tang, C Fan, C Zhang, X He and Y He. An overview on limitations of TiO2-based particles for photocatalytic degradation of organic pollutants and the corresponding countermeasures. *Water Res.* 2015; **79**, 128-46.

[17] W Buraso, V Lachom, P Siriya, and P Laokul. Synthesis of TiO_2 nanoparticles via a simple precipitation method and photocatalytic performance. *Mater. Res. Exp.* 2018; **5**, 115003.

[18] C Marien, C Marchal, A Koch, D Robert and P Drogui. Sol-gel synthesis of TiO_2 nanoparticles: Effect of Pluronic P123 on particle's morphology and photocatalytic degradation of paraquat. *Environ. Sci. Pollut. Res.* 2017; **24**, 12582-8.

[19] L Mardiana, AYP Wardoyo, Masruroh and HA Dharmawan. Synthesis TiO_2 using sonochemical method and responses the CO_2 gas of the nanoparticle TiO_2 layers on the QCM sensor surfaces. *J. Phys. Conf. Ser.* 2022; **2165**, 012014.

[20] MP Izaak, YE Gunanto, H Sitompul and WA Adi. The synthesis of TiO_2 nanoparticles by milling and coprecipitation mixed method. *Jurnal Fisika Dan Aplikasinya* 2020; **16**, 67-70.
[21] N Rab, FK Chong, HI Mohamed and WH Lim. Preparation of TiO_2 nanoparticles by hydrolysis of $TiCl_4$ using water and glycerol solvent system. *J. Phys. Conf. Ser.* 2018; **1123**, 012065.
[22] VM Ramakrishnan, M Natarajan, A Santhanam, V Asokan and D Velauthapillai. Size controlled synthesis of TiO_2 nanoparticles by modified solvothermal method towards effective photo catalytic and photovoltaic applications. *Mater. Res. Bull.* 2018; **97**, 351-60.
[23] GS Falk, M Borlaf, MJ López-Muñoz, JC Fariñas, JBR Neto and R Moreno. Microwave-assisted synthesis of TiO_2 nanoparticles: Photocatalytic activity of powders and thin films. *J. Nanopart. Res.* 2018; **20**, 23.
[24] EK Tetteh, S Rathilal, D Asante-Sackey and MN Chollom. Prospects of synthesized magnetic TiO_2-based membranes for wastewater treatment: A review. *Materials* 2021; **14**, 3524.
[25] MC Kimling and RA Caruso. Sol-gel synthesis of hierarchically porous TiO_2 beads using calcium alginate beads as sacrificial templates. *J. Mater. Chem.* 2012; **22**, 4073-82.
[26] G Calcagno, A Lotsari, A Dang, S Lindberg, AEC Palmqvist, A Matic and C Cavallo. Fast charging negative electrodes based on anatase titanium dioxide beads for highly stable Li-ion capacitors. *Mater. Today Energ.* 2020; **16**, 100424.
[27] G Tóth, F Bugyi, S Sugár, G Mitulović, K Vékey, L Turiák and L Drahoss. Selective TiO_2 phosphopeptide enrichment of complex samples in the nanogram range. *Separations* 2020; **7**, 74.
[28] PS Bakshi, D Selvakumar, K Kadirvelu and NS Kumar. Chitosan as an environment friendly biomaterial - a review on recent modifications and applications. *Int. J. Biol. Macromol*. 2020; **150**, 1072-83.
[29] VP Santos, NSS Marques, PCSV Maia, MABD Lima, LO Franco and GMD Campos-Takaki. Seafood waste as attractive source of chitin and chitosan production and their applications. *Int. J. Mol. Sci.* 2020; **21**, 4290.
[30] A Wozniak and M Biernat. (2022), Methods for crosslinking and stabilization of chitosan structures for potential medical applications. *J. Bioactive Compat. Polym.* 2022; **37**, 151-67.
[31] C Tiloke, A Phulukdaree and AA Chuturgoon. *The chemotherapeutic potential of gold nanoparticles against human carcinomas: A review*. *In*: AM Holban and AM Grumezescu (Eds.). Nanoarchitectonics for smart delivery and drug targeting. William Andrew, New York, 2016, p. 783-811.
[32] M Thommes, K Kaneko, A Neimark, JP Olivier, F Rodriguez-Reinoso, J Rouquerol and KSW Sing. Physisorption of gases, with special reference to the evaluation of surface area and pore size distribution (IUPAC technical report). *Pure Appl. Chem.* 2015; **87**, 1051-69.
[33] H Kaur, S Kumar, NK Verma and P Singh. Role of pH on the photocatalytic activity of TiO_2 tailored by W/T mole ratio. *J. Mater. Sci. Mater. Electron.* 2018; **29**, 16120-35.
[34] P Atkins. *Physical chemistry*. Oxford University Press, London, 1999.